

## Use of Low-Temperature Scanning Electron Microscopy to Compare and Characterize Three Classes of Snow Cover

JAMES FOSTER, RICHARD KELLY,\* ALBERT RANGO,† RICHARD ARMSTRONG,‡ ERIC F. ERBE,§ CHRISTOPHER POOLEY,¶ WILLIAM P. WERGIN§

Laboratory for Hydrospheric and Biospheric Sciences, NASA Goddard Space Flight Center, Greenbelt; \*Department of Geography, Waterloo University, Waterloo, Canada; †Jornada Experimental Range, Agricultural Research Service (ARS), U. S. Department of Agriculture (USDA), New Mexico State University, Las Cruces, New Mexico; ‡National Snow and Ice Data Center, University of Colorado, Boulder, Colorado; §Soybean Genomics and Improvement Laboratory and ¶Hydrology and Remote Sensing Laboratory, ARS, USDA, Beltsville, Maryland, USA

**Summary:** This study, which uses low-temperature scanning electron microscopy (LTSEM), systematically sampled and characterized snow crystals that were collected from three unique classes of snow cover: prairie, taiga, and alpine. These classes, which were defined in previous field studies, result from exposure to unique climatic variables relating to wind, precipitation, and air temperature. Snow samples were taken at 10 cm depth intervals from the walls of freshly excavated snow pits. The depth of the snow pits for the prairie, taiga, and alpine covers were 28, 81, and 110 cm, respectively. Visual examination revealed that the prairie snow cover consisted of two distinct layers whereas the taiga and alpine covers had four distinct layers. Visual measurements were able to establish the range of crystal sizes that occurred in each layer, the temperature within the pit, and the snow density. The LTSEM observations revealed the detailed structures of the types of crystals that occurred in the snow covers, and documented the metamorphosis that transpired in the descending layers. Briefly, the top layers from two of the snow covers consisted of freshly fallen snow crystals that could be readily distinguished as plates and columns (prairie) or graupel (taiga). Alternatively, the top layer in the alpine cover consisted of older dendritic crystal fragments that had undergone early metamorphosis, that is, they had lost their sharp edges and had begun to show signs of joining or bonding with neighboring crystals. A unique layer, known as sun crust, was found in the prairie snow cover; however, successive samplings from all three snow

covers showed similar stages of metamorphism that led to the formation of depth hoar crystals. These changes included the gradual development of large, three-dimensional crystals having clearly defined flat faces, sharp edges, internal depressions, and facets. The study, which indicates that LTSEM can be used to enhance visual data by systematically characterizing snow crystals that are collected at remote locations, is important for understanding the physics of snowpacks and the metamorphosis that leads to potential avalanche situations. In addition, the metamorphosis of snow crystals must be considered when microwave radiometry is used to estimate the snow water equivalent in the winter snowpack, because large snow crystals more effectively scatter passive microwave radiation than small crystals.

**Key words:** snow crystal, snow cover, depth hoar, low-temperature scanning electron microscopy

**PACS:** 61.16 BG, 61.66.-f, 81.10Aj, 92.40.Rm

### Introduction

The winter snow cover is comprised of snow crystals that with time undergo considerable structural changes referred to as metamorphoses, a complex process that is influenced by the topography of the land, internal pressure effects, and local climatic factors such as sun exposure, temperature variability, precipitation rates, and wind history (Sturm *et al.* 1995, UNESCO/IASH/WMO 1970). Using simple optical instruments, researchers have described distinct types of snow covers, which are based upon the structural features of the metamorphosed crystals that they contain.

Through the years, various classification systems have been proposed in an attempt to understand, characterize, and classify the types of snow covers that are found worldwide. One of the most recent systems is that proposed

---

Address for reprints:

William P. Wergin  
Soybean Genomics and Improvement Laboratory  
Agricultural Research Service  
U.S. Department of Agriculture  
Beltsville, MD 20705, USA  
e-mail: wwergin@msn.com

by Sturm *et al.* (1995), who used climatic factor analysis to propose a seasonal snow cover classification system that would apply to local as well as global situations. In their system, snow covers are grouped into six classes: tundra, taiga, alpine, maritime, prairie, and ephemeral. Each class, which has unique textural and stratigraphic features, includes visual descriptions of snow crystal morphology. However, the structural details of crystal morphology are somewhat compromised by the optical techniques that are used in the field to characterize the snow crystals.

During the past decade, low-temperature scanning electron microscopy (LTSEM) has been used to examine crystals of snow and ice (see review, Wergin *et al.* 2003). Using this technique, samples have been collected in the field and shipped to a laboratory by common air carrier from distances as far as 5,000 miles (Erbe *et al.* 2003). Delicate specimens of snow crystals and ice grains survive the collection and shipment procedures and have been stored for more than 3 years without undergoing any visible structural changes. With this technique, the samples are not subjected to melting or sublimation artifacts. The LTSEM allows individual crystals to be observed for several hours with no detectable changes. Furthermore, the resolution of the instrument permits recording of photographs depicting the true shapes of snowflakes, snow crystals, snow clusters, ice grains, and interspersed air spaces. This technique has been successfully used to describe fresh precipitating snow (Rango *et al.* 1996a, 2003; Wergin and Erbe 1994a, b, c; Wergin *et al.* 1995, 1996a, 2002; Wolff and Reid 1994) and metamorphosed snow (Dominé *et al.* 2003; Foster *et al.* 1996; Rango *et al.* 1996b; Wergin *et al.* 1996a, b, c, 2003).

However, gaining a better understanding of snow physics, as well as the impact and interactions of seasonal snow with other components of the Earth system, such as cycling of water and energy, requires more systematic and detailed studies of snow crystal metamorphoses. For example, global snow water equivalent (SWE) is an important water storage component of the hydrological cycle and a major source of water storage and runoff in many parts of the world. Melting snow contributes upward of 70% of the total annual water supply in the western U.S (Rango *et al.* 1989). In the Hindu Kush Himalayas, snow and ice melt is a vital resource for approximately 500 million people in surrounding countries. Therefore, more accurately characterizing snow covers, especially at local and regional scales, would be useful to water managers.

To gain a greater understanding of snow crystal metamorphism that occurs in snow covers and to determine how it may relate to estimations of SWE, the current study sampled snow from three classes of snow covers: prairie, taiga, and alpine. Snow samples from each of these classes were systematically collected, measured and characterized in the field. In the laboratory, LTSEM was used to describe the structural details of snow crystals that were found within each of these snow covers.

## Materials and Methods

### Sampling Sites

During the 2002 NASA Cold Land Processes Field Experiment (CLPX) in Colorado, Intensive Study Area (ISA) snow pits were excavated and analyzed using traditional field methods to quantify snow stratigraphy (particularly snow grain size), snow density, and snow temperature in the vertical profile. Snow samples for LTSEM analyses were collected from a snow pit in each of three different ISAs. Each pit for LTSEM sampling was adjacent to a selected pit used for the traditional analyses. In some cases, the LTSEM sample pit face was an extension of the pit face used for the traditional analysis. Both traditional pit analysis and LTSEM sampling were conducted at nearly the same time, enabling both methods to be compared. Full details of pit measurement data sets for the CLPX campaign are described in Cline *et al.* (2002).

*Prairie snow cover:* The Illinois River ISA, which represents prairie snow cover, was located in the North Park, Mesocell Study Area (MSA). The area consisted of patchy snow and bare ground (sage brush—steppe vegetation). For LTSEM sampling, a 28 cm pit was excavated near the Illinois River, 300 m west and below the National Wildlife Refuge parking area. Samples were taken from the north wall of the pit at 10 cm intervals and from the snow surface. At the time of collection, the air temperature was  $-4.5^{\circ}\text{C}$ .

*Taiga snow cover:* The Frasier MSA, which represents taiga snow cover, was located at the Alpha Sector of the ISA, southeast of a young coniferous (predominantly spruce-fir) and deciduous forest. For LTSEM sampling, an 81 cm pit, representing average snow cover, was excavated. Samples were taken from the north wall of the pit at 10 cm intervals beginning at the base of the pit. At the time of collection, the air temperature was  $-3^{\circ}\text{C}$  and light graupel was falling.

*Alpine snow cover:* The Rabbit Ears MSA represented an alpine snow cover. The pit site consisted of an open alpine mountain terrain (alpine meadows) with interspersed coniferous and Aspen groves. For LTSEM sampling, a 110 cm pit, representing average snow cover, was dug in the Charlie Sector. Samples were taken from the north wall at 10 cm intervals beginning at the base of the pit. At the time of collection, the air temperature was  $-4^{\circ}\text{C}$ .

### Sampling Procedures

Details for sampling snow crystals and ice grains were according to procedures recently published by Erbe *et al.* (2003). Briefly, all samples of snow and ice were collected on sampling plates that were fabricated in the laboratory. The plates, which were cut from sheets of stock copper 1.5 mm thick, measured  $15 \times 29$  mm. At the sampling site, a plate was coated with a thin layer of a liquid cryoadhesive (Tissue-Tek). The cryoadhesive and the plates were cooled

to temperatures at or slightly below freezing. Immediately after a specimen was collected, the plate containing the cryoadhesive and the sample was plunged into a vessel of liquid nitrogen ( $\text{LN}_2$ ). In all subsequent procedures, including shipping, storing, coating, observing, and photographing, the plates containing the samples were maintained at near  $\text{LN}_2$  temperatures ( $-196^\circ\text{C}$ ). At these temperatures, the vapor pressure of water was not significant and sublimation did not occur at a detectable rate. Furthermore, recrystallization of pure water-ice does not occur (Beckett and Read 1986) and fully frozen and hydrated samples remain stable for hours while being observed with the LTSEM (Wergin and Erbe 1991).

To collect samples from snow pits, a precooled ( $\text{LN}_2$ ) scalpel was used to dislodge snow crystals gently from a freshly excavated pit wall. The crystals were deposited on the cryoadhesive-coated plate, which was rapidly plunged into  $\text{LN}_2$ . To collect tightly bonded snow crystals from their native site, an  $\text{LN}_2$ -cooled scalpel blade was used to dislodge grain clusters from the pit wall. The clusters were collected onto a plate containing the cryoadhesive and then cooled to  $\text{LN}_2$  temperature. This technique was also used to sample sun crust and depth hoar, which existed in the stratified layers of the snow pit.

Fracturing snow clusters was used to reveal the extent of internal air spaces and details of bonding. Fracturing was accomplished in the prechamber of the LTSEM by using a pick to remove randomly a portion of the snow cluster or ice sample. This process exposed a pristine internal fractured surface that was then coated and imaged in the LTSEM.

### Shipping and Storing Samples

At the collection site, a forceps was used to insert plates diagonally into square brass tubing,  $13 \times 13$  mm, inside diameter. The tubes containing the sampling plates were lowered into a lightweight dry shipping Dewar or Cryopak shipper (Taylor Wharton, Theodore, Ala., USA) that had been previously cooled with  $\text{LN}_2$ . The Dewar was carried from the collection site and then either transported by vehicle or sent by priority air express to our laboratory in Beltsville, Md. The shipper, which is designed to maintain  $\text{LN}_2$  temperatures for a minimum of 21 days when properly precooled, has been previously used to transport samples from numerous locations including remote regions of Washington, North Dakota, and Alaska. Upon reaching the laboratory, the samples were transferred to an  $\text{LN}_2$  storage Dewar where they remained until being further prepared for observation with LTSEM.

### Coating Samples

To prevent charging, frozen samples were coated with 2 to 10 nm of platinum by using a magnetron sputtercoating device in a high-purity argon environment within the prechamber of the cryosystem.

### Recording Images in the Scanning Electron Microscope

The commercial specimen holder, which was supplied with the cryosystem, was modified to accommodate the sampling plates (Erbe *et al.* 2003). For observation, the specimen holder containing the plate was inserted into a Hitachi S-4100 field emission scanning electron microscope (SEM) (Hitachi High-Technology Corp., Tokyo, Japan) equipped with an Oxford CT 1500 HF Cryo-system (Oxford Instruments, Enysham, England). The cold stage was maintained at  $-130^\circ$  to  $-185^\circ\text{C}$ . Accelerating voltages of 500V to 10 kV were used to observe the samples. The samples were imaged for as long as 2 h without observing any changes in the structural features or in the coating integrity on the snow crystals or ice grains. Selected images were recorded onto Polaroid Type 55 P/N film (Polaroid, Cambridge, Mass., USA).

## Results

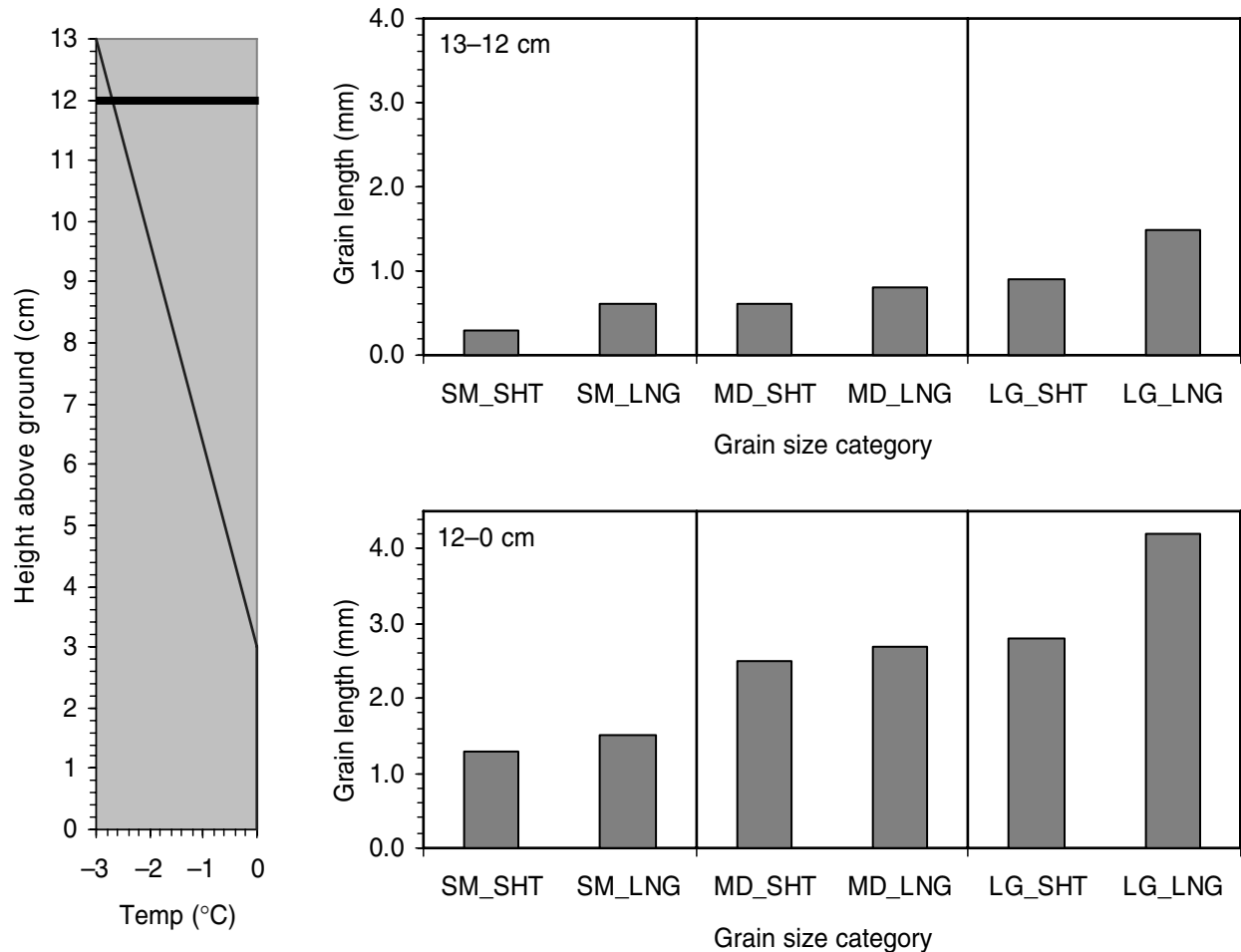
### Prairie Snow Cover

*Field characterization of the snow pit (see Table 1):* The prairie site at Illinois River ISA (site NISP16 at UTM Zone 13, coordinate  $39.45^\circ\text{E}$ ,  $45.06^\circ\text{N}$ ) in the North Park, Mesocell Study Area (MSA) was sampled at 15:20 h on February 21, 2002. The traditional pit analysis measured a snow depth of 13 cm and a snow water equivalent (SWE) of 32 mm. At this location, the snow cover was variable and could not support the measurement of snow density profiles. Therefore, snow density was measured as a single integrated value and repeated three times. The average snow density for the Illinois River site was  $244\text{ kg m}^{-3}$  with a standard deviation of  $13\text{ kg m}^{-3}$ . The measured surface temperature was  $-3^\circ\text{C}$  increasing to  $0^\circ\text{C}$  at 0–3 cm above the underlying ground surface. Two snow layers were observed: a lower layer from the snow–ground interface to 12 cm and an upper layer from 12 cm to the snow–air interface. Grain axis sizes in the upper layer averaged 0.8 mm with a standard deviation of 0.4 mm. In the lower layer, the average grain size was 2.5 mm with a standard deviation of 1.0 mm. These statistics represent the combined small, medium, and large crystal statistics for both short and long axes of measurement.

*Low-temperature SEM characterization:* The layer of newly fallen snow consisted largely of discrete hexagonal plates and capped columns as well as fragments and variations of these classes (Fig. 1a). Most of the intact crystals were in the 0.5 to 0.8 mm range and exhibited no significant bonding.

A sun crust layer, which consisted of tightly bonded crystals, was found beneath the newly fallen snow. This layer was broken into small clusters for mounting on the sample plate. In this layer, the individual crystals, which measured from 0.8 to 1.2 mm, lacked the discrete edges found in the newly fallen snow (Fig. 1b). Alternatively, these crystals

TABLE I Illinois River (North Park) data for February 21, 2002 (Site label: NISP16). The left hand line graph represents the temperature variation with snow depth where 0 cm is the snow-ground interface and 13 cm is the snow surface. In all three Tables, the bar charts on the right represent long and short axes (LNG and SHT, respectively) grain size measurements for small, medium and large snow crystals (SM, MD and LG, respectively) in each stratigraphic layer. For example, medium-sized crystals, long axis would be termed MD\_LNG. The stratigraphic layer, to which each bar chart refers is identified in the top left inside corner of that chart.



lacked crisp edges, exhibited some rounding, and were tightly bonded. Flat surfaces, other than those resulting from breaking the clusters, were rarely encountered.

Below the layer of sun crust, the samples consisted of crystals that were less tightly bonded. Distinct crystals beginning to exhibit flat faces as well as considerable rounding were apparent (Fig. 1c). The sizes of the crystals were not significantly different from those found in the sun crust layer; however, their features were characteristic of the early stages of depth hoar formation.

The base of the snowpack was composed of large depth hoar crystals. These crystals, which commonly measured 2 to 4 mm across, were considerably larger than those from any of the upper layers (Fig. 1d). They generally exhibited flat surfaces with well-defined edges along the vertical or c-axis. Alternatively, examination of the horizontal (a-axis) surfaces revealed a series of facets or steps that receded as one moved from the edge to the center of the crystal.

### Taiga Snow Cover

*Field characterization of the snow pit (see Table II):* At Fraser MSA, traditional snow pit measurements at the St. Louis Creek, Taiga ISA (site FSSP09, UTM coordinate 42.46° E, 44.20° N) were conducted at 13:25 h on February 20, 2002. The total snow depth was 85 cm with a SWE of 167 mm. Four distinct layers were observed in the field with boundaries at 25, 43, and 67 cm above the ground. Snow density progressively increased from 82 kg m<sup>-3</sup> in the upper layer to 227 kg m<sup>-3</sup> and 230 kg m<sup>-3</sup> in the middle two layers, and 239 kg m<sup>-3</sup> at the base. Snow temperature decreased from -3° C at the snow-air interface to -5° C in the second layer from the snow-air interface and then steadily increased to -1° C at the base of the snowpack. Grain size measurements were not available for the uppermost stratigraphic layer. For the second layer below the surface, between 67 and 43 cm above the ground, the average grain size was

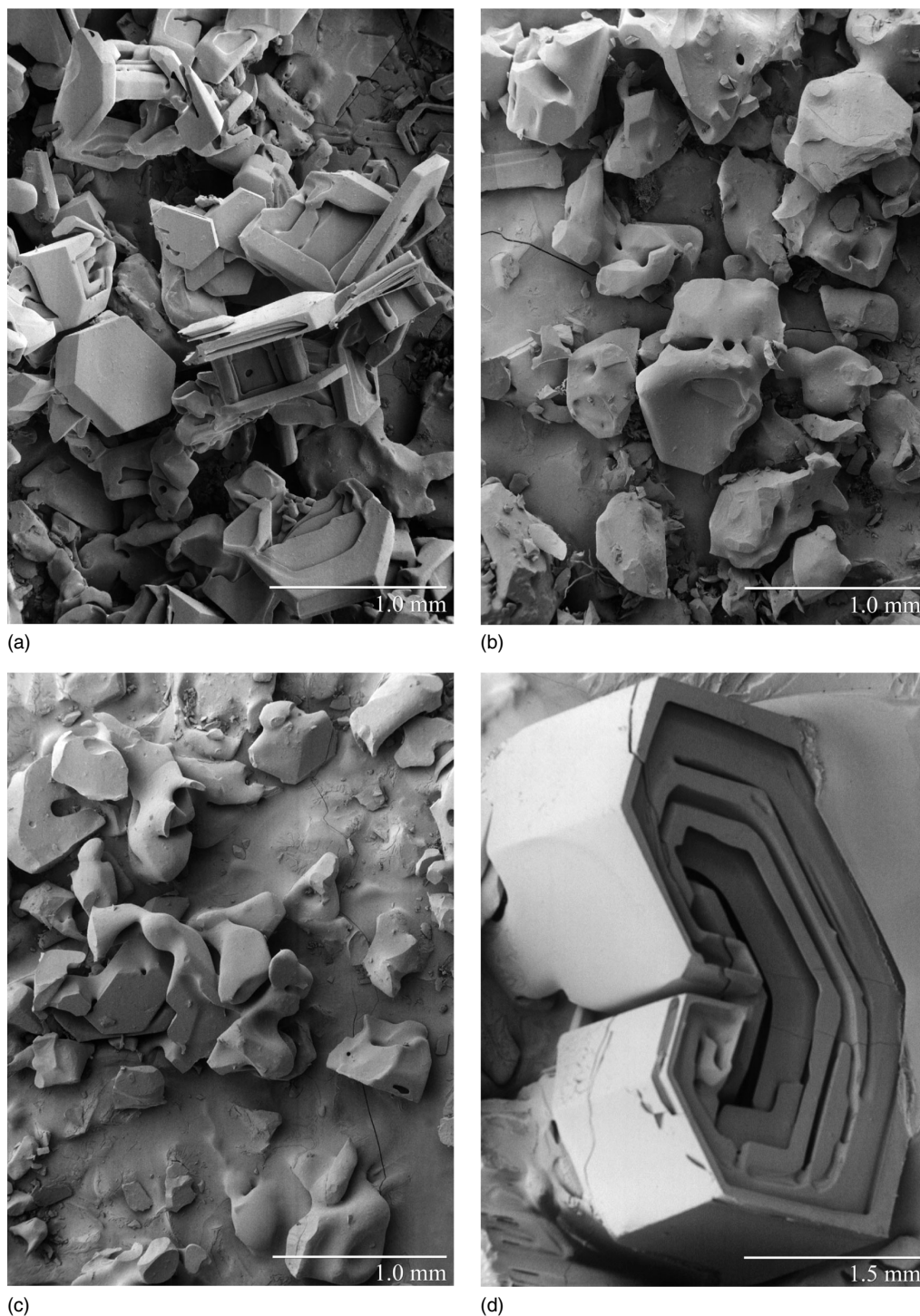
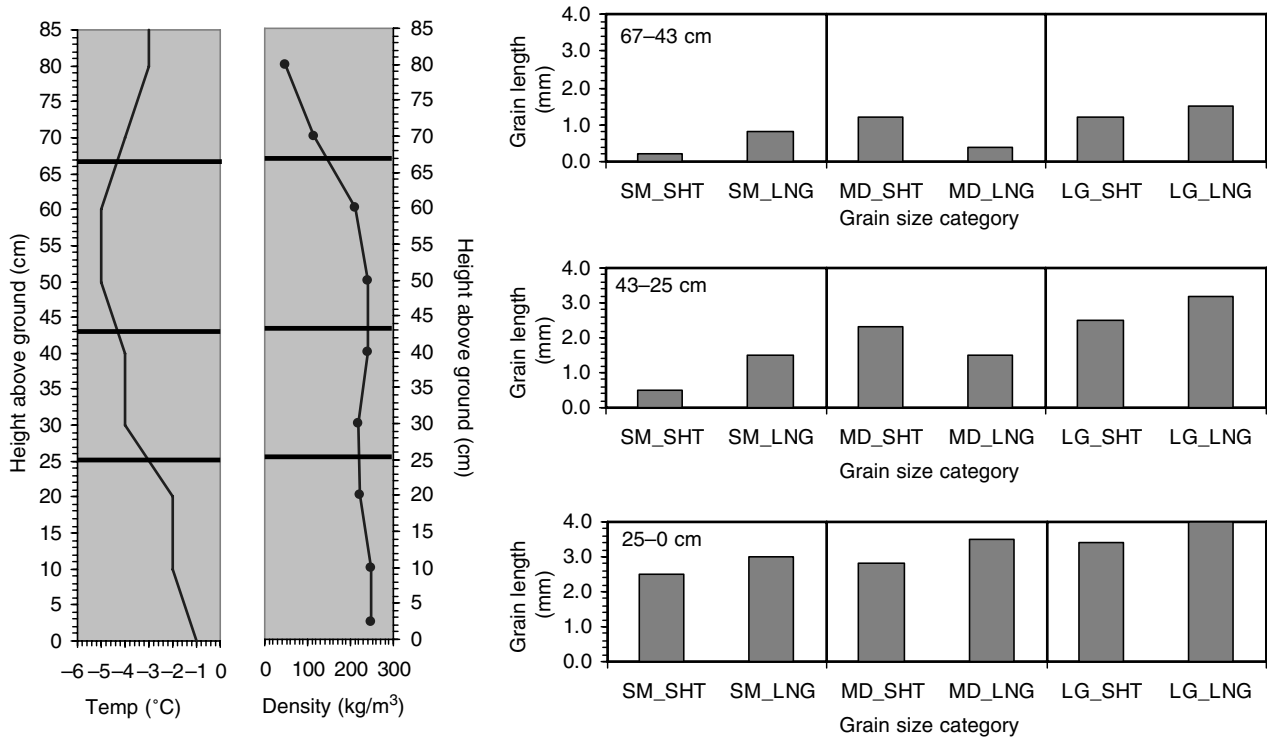


FIG. 1 Samples of newly fallen snow crystals collected from the Illinois River site (Prairie Snow Cover). (a) Samples from the surface of the snowpack largely consisted of hexagonal plates and capped columns having discrete edges and showed minimal signs of metamorphosis. The majority of the crystals measured 0.5 to 0.8 mm and exhibited no significant bonding. (b) Sample of the sun crust layer taken 25 cm above ground level. This layer, which consisted of old, tightly bonded crystals that formed a sun crust, was broken into small clusters for mounting and observation. The crystals in this layer measured from 0.8 to 1.2 mm and lacked the discrete edges characteristic of crystals from newly fallen snow [see a]. (c) Samples from below the layer of sun crust contained crystals that were less bonded. Distinct crystals in this layer exhibited flat and rounded faces. No significant growth in the size of the crystals was evident. These crystals are believed to represent the early stages of depth hoar formation. (d) Samples from 5 cm above ground level consisted of large, distinct crystals commonly known as depth hoar crystals. These crystals, which commonly measured 2 to 4 mm across, generally had flat vertical faces, but their horizontal faces exhibited a series of steps or facets that receded toward the center of the crystal.

TABLE II St. Louis Creek (Fraser) data for February 20, 2002 (Site label: FSSP09). The far left hand line graph represents the temperature variation with snow depth where 0 cm is the snow-ground interface and 85 cm is the snow surface. The second line graph to the right represents snow density variations through the profile. The solid horizontal lines represent boundaries between discrete stratigraphic layers. No grain size data exist for the uppermost layer.



0.9 mm with a standard deviation of 0.5 mm. At 43 to 25 cm above the ground, the snow grain size average and standard deviation was 1.9 and 0.9 mm, respectively, and in the basal layer grain sizes averaged 3.2 mm with a standard deviation of 0.5 mm.

*Low-temperature SEM characterization:* The surface of the snow cover at this site had a fresh layer of crystals consisting of graupel, commonly referred to as snow pellets or soft hail. The majority of the graupel crystals frequently exceeded 1.0 mm in length (Fig. 2a). A layer of dendritic snow crystals, 10 cm deep, was found below the graupel (Fig. 2b). Occasionally, a dendrite, which characteristically has 6 arms, was intact; however, in most cases only fragments consisting of the dendritic arms were apparent. The surfaces of the dendritic crystals were not sharply defined but were more sinuous or somewhat rounded, indicating an early stage of metamorphosis.

A 2- to 3-day old layer, which was found 11 to 19 cm below the surface, also exhibited intact dendritic crystals, dendritic arms, and early formations of bonded snow grains. Crystals, which retained the general characteristics of dendrites, exhibited more rounding than those in the snow layer above (Fig. 2c). Crystals, which had lost most of their dendritic characteristics, were bonded and measured 0.5 to 1.0 mm across (Fig. 2d).

The final layer of the snowpack, 44 to 81 cm below the surface, was visually characterized as “faceted depth hoar.”

This layer was sampled at 55, 65, and 75 cm in an attempt to illustrate the successive stages of metamorphosis that had occurred in the Taiga snow cover. At 55 cm, the crystals were more three-dimensional than the dendritic forms that were found above and frequently approached 1 mm in length and width (Fig. 2e). They were generally bonded; their external surfaces occasionally exhibited flat faces with sharply defined edges as well as more rounded surfaces. Small depressions or holes were frequently apparent in the crystals.

At a depth of 65 cm, the crystals frequently exceeded 3 to 4 mm in length. Bonding with neighboring crystals was generally evident. The crystal faces were more frequently flat with sharply defined edges and central depressions, which correspond to the cup-like features characteristic of depth hoar crystals (Fig. 2f).

Finally, at 75 cm below the surface, large, three-dimensional depth hoar crystals frequently measuring 4 mm were found (Fig. 2 g,h). These crystals generally had sharp angular external surfaces but varied greatly in their shapes. Most of them were only lightly bonded but typically exhibited steps or facets and had a depressed central core.

### Alpine Snow Cover

*Field characterization of the snow pit (see Table III):* For the Rabbit Ears MSA, a snow pit was excavated at the Walton Creek Alpine ISA site (RWSP14) located at UTM coordinate

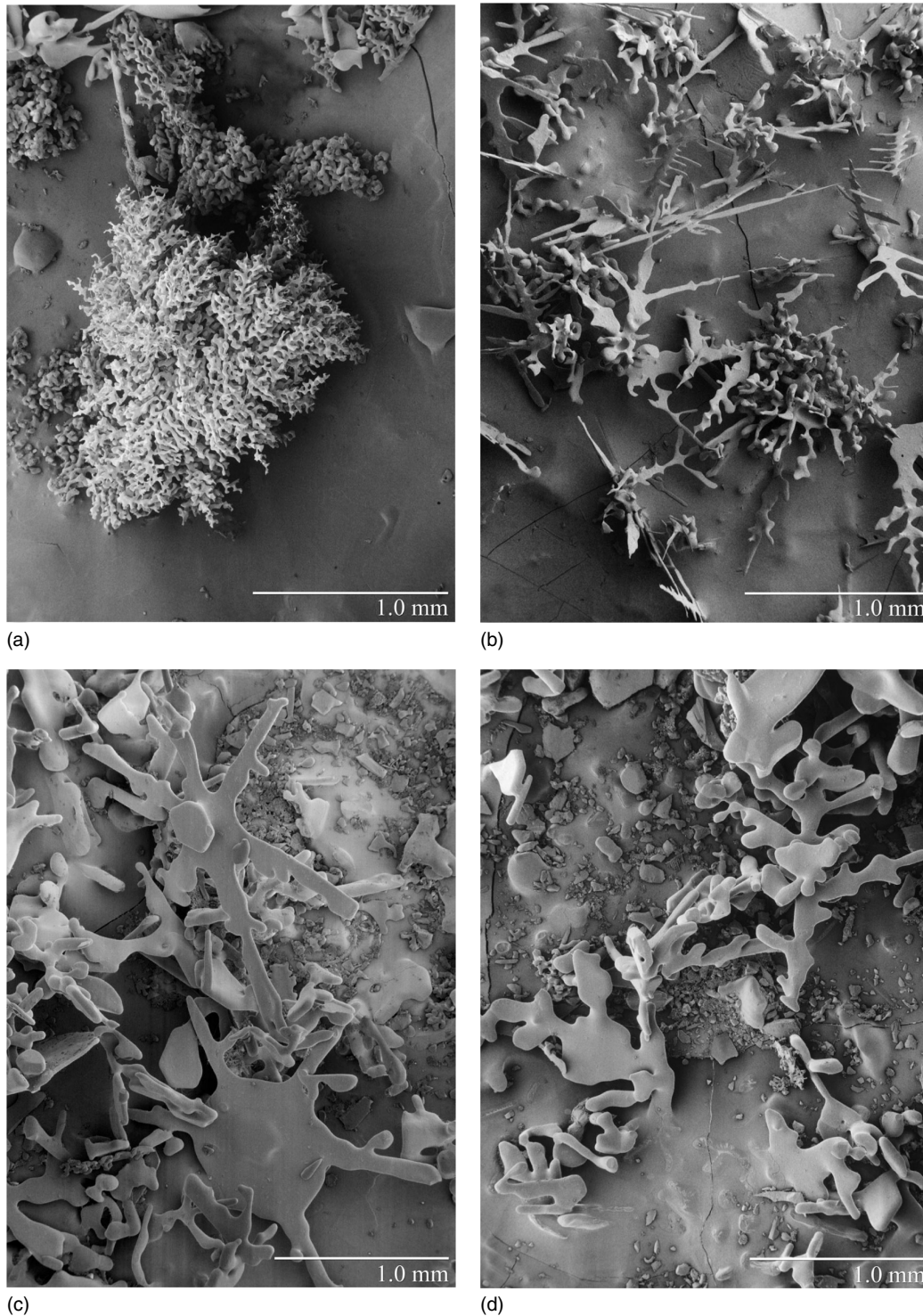


FIG. 2 Samples of snow crystals collected from the Saint Louis Creek site (Taiga Snow Cover). (a) Example of graupel particle found on the surface of the snowpack. The shape of the original snow crystal cannot be determined because of the hundreds of frozen cloud droplets that have frozen to its surface. Graupel particles frequently exceed 1.0 mm in length. (b) Sample from the 10 cm layer of new snow that lies beneath the graupel. Occasionally intact dendritic crystals were found, but generally this layer consisted of fragments or “arms.” The edges of these crystals are not sharply defined but exhibit rounding indicative of an early stage of metamorphosis. (c) and (d) Samples from the 2- to 3-day old layer that is found 11 to 19 cm below the surface. Two types of metamorphosed crystals are found in this layer: those that can be identified as intact dendrites or dendritic fragments (c) and other more sinuous forms that are joined or bonded (d). The dendritic forms exhibit considerably more rounding than is observed in the crystals from the upper layer. The bonded grains generally appear as relatively flat, amorphous structures measuring 0.5 to 1.0 mm.

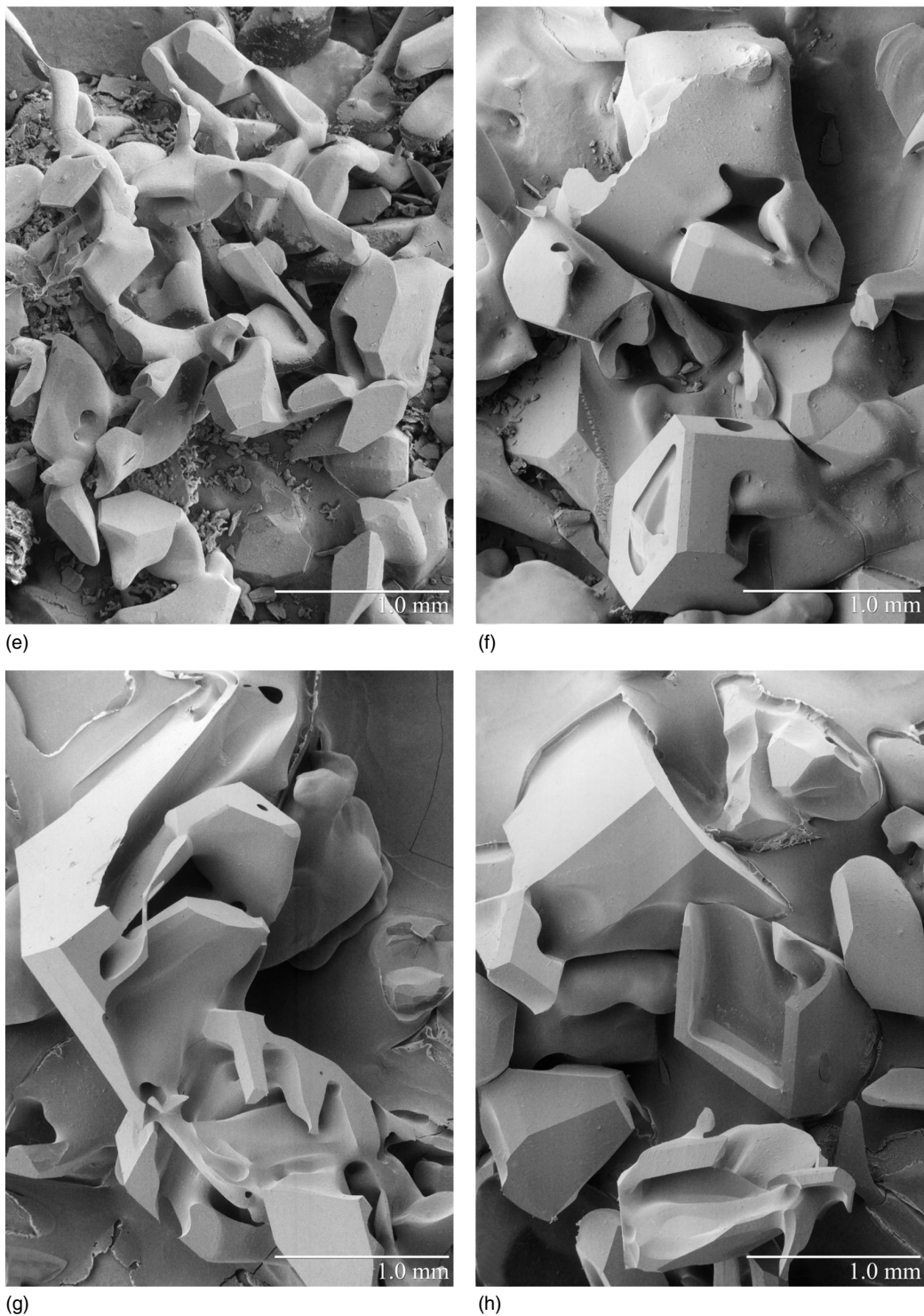
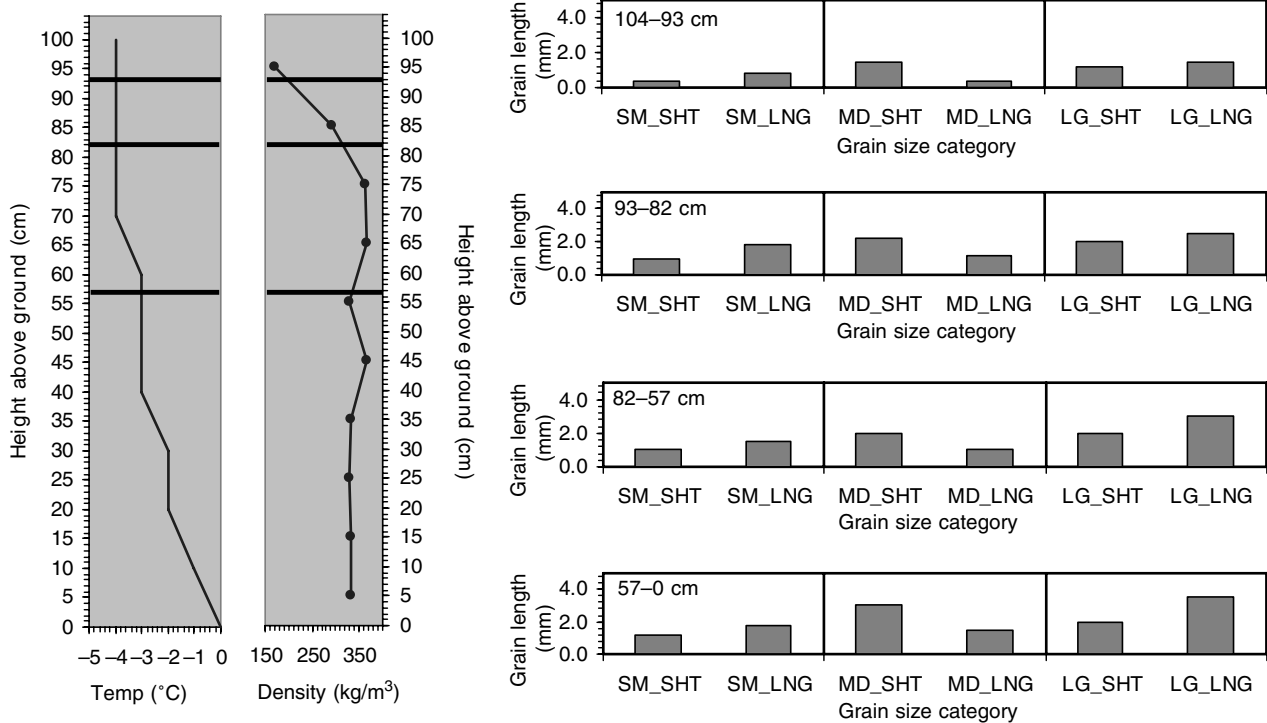


FIG. 2 (continued) (e) Sample of snow taken from 55 cm below the surface. The crystals in this layer are more three-dimensional than the dendritic forms that were found above. They frequently approach 1 mm in length, are generally bonded or joined, and their external surfaces exhibit both flat faces with sharply defined edges and more rounded amorphous surfaces. (f) Sample of snow taken at 65 cm below the surface. At this level, the snow crystals frequently exceeded 1 mm in length and width. The adjacent crystals are frequently joined or bonded. The faces of the crystals are generally flat with sharply defined edges. Shallow depressions, probably corresponding to the cup-like features characteristic of depth hoar crystals, are beginning to form. (g) and (h) Sample of snow taken at 75 cm below the surface. At this level, the crystals are more three-dimensional and larger than those found in the layers above and frequently measure 2 to 3 mm. These crystals, which correspond to the depth hoar crystals described in optical studies, generally have flat external faces and exhibit "steps" or facets and a depressed central core or cup, which is characteristic of depth hoar crystals.



TABLE III Walton Creek (Rabbit Ears) data for February 24, 2002 (Site label: RWSP14). The far left hand line graph represents the temperature variation with snow depth where 0 cm is the snow–ground interface and 104 cm is the snow surface. The second line graph to the right represents snow density variations through the profile. The solid horizontal lines represent boundaries between discrete stratigraphic layers.



36.03° E, 44.74° N. Traditional measurements were conducted at 13:25 h on February 24, 2002. The total snow depth was 104 cm with a SWE of 321 mm. Four distinct layers were observed in the field with boundaries at 93, 82, and 57 cm above the ground. Snow density increased from the surface to the base. At the surface, density was  $171 \text{ kg m}^{-3}$  in the upper zone. In the next layer from the top, the density was  $291 \text{ kg m}^{-3}$ , increasing to a maximum of  $364 \text{ kg m}^{-3}$  in the layer between 82 and 57 cm from the base. The bottom layer had an average density of  $337 \text{ kg m}^{-3}$ . Snow temperature was between  $-4^\circ \text{C}$  and  $-3^\circ \text{C}$  in the uppermost three layers and increased to  $0^\circ \text{C}$  at the base of the snowpack. The average snow grain sizes gradually increased toward the base of the snowpack. The surface layer average and standard deviation values were 1.0 and 0.5 mm, respectively. The second and third layers from the snow–air interface had average grain sizes of 1.8 mm with a slight difference in standard deviation (0.6 mm for the 93–92 cm layer and 0.8 mm for the 82–57 cm layer). The basal snow layer had an average grain size of 2.2 mm and a standard deviation of 0.9 mm.

*Low-temperature SEM characterization:* At 5 cm below the surface, the snow samples consisted of dendritic fragments which lacked sharply defined edges (Fig. 3a). The crystals were rounded and exhibited some bonding. Ten cm below this layer, none of the basic crystalline forms, that is, dendrites, plates, columns, or needles, were apparent. Alternatively, this layer consisted of crystals that had become more three-dimensional

and heterogenic in structure; no single, discrete shape prevailed (Fig. 3b). The crystals lacked discrete edges. In addition, bonding between adjacent crystals was readily apparent.

Samples collected from 25 cm below the surface exhibited characteristics of the early forms of depth hoar. The crystals were larger, measuring 0.8 to 1.2 mm, and some bonding had occurred (Fig. 3c). Although no distinct flat faces had formed, depressions or holes were occasionally observed near in the centers of the crystals.

From 35 to 65 cm below the surface, the general appearance of the crystals did not change significantly. The most noticeable change was continued growth, resulting in depth hoar crystals that ranged from 1 to 2 mm at 65 cm below the surface. In addition, the faces of crystals became more flattened with descending depth (Fig. 3d). From 75 to 105 cm below the surface, the crystals consisted of classical depth hoar (Fig. 3e,f). Faceting became more prominent, the crystals appeared to be only weakly bonded and dimensions were in the 1 to 3 mm range.

## Discussion

### Historical Background and Terminology

Numerous studies have noted the wide diversity that exists in the structure of snow. As a result, investigators

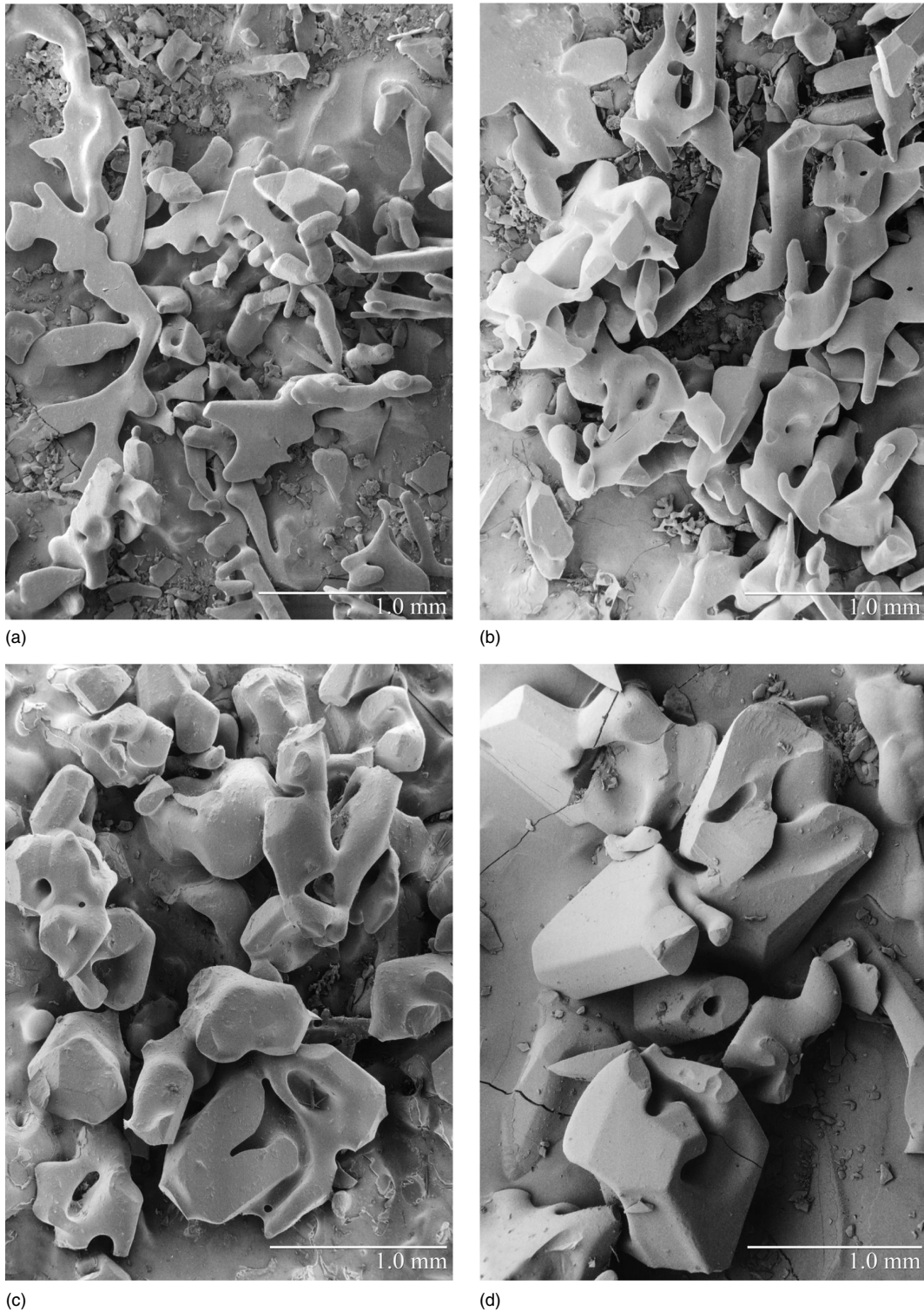


FIG. 3 Samples of snow crystals collected from the Walton Creek site (Alpine Snow Cover). (a) Sample from the 5 cm below the surface of the snow cover. At this level the crystals consist of dendrites and dendritic fragments or arms that exhibit no sharply defined edges. (b) At 15 cm below the surface, no classical crystalline shapes are apparent. Alternatively, the crystals that are found tend to be more three-dimensional and heterogeneous in their forms. Their edges have become rounded and the amorphous shapes indicate that bonding of adjacent crystals has occurred. (c) Twenty-five cm below the surface, larger crystals exhibiting bonding are prevalent. The crystals are amorphous, do not exhibit flat faces, but occasionally contain depressions or holes (arrows). These forms represent the early stages of depth hoar formation. (d) Further growth of the depth hoar crystals is evident in samples taken 35 to 65 cm below the surface. As a result, crystals range from 1 and 2 mm across and exhibit more flattened faces.

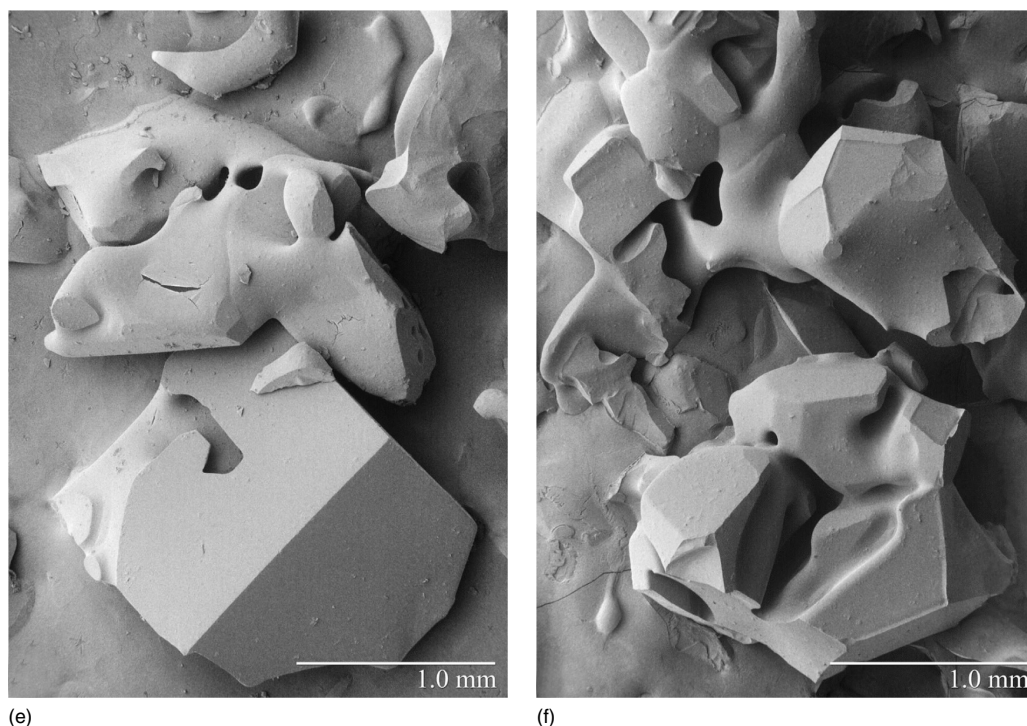


FIG. 3 (continued) (e) and (f) At 75 to 105 cm below the samples are composed of classical depth hoar crystals. They have sharply defined flat faces with depressions that reflect the internal faceting that generally exists in depth hoar. The crystals appear to be only weakly bonded and dimensions remain in the 1 to 2 mm range.

using light microscopy, hand lenses, and macrophotography have proposed classification schemes of the various forms of snow crystals that are found in fresh and metamorphosed snow. These efforts began over 100 years ago when Hellman (1893) and Nordenskiöld (1893) independently observed that fresh falling snow occurred in two basic forms, namely columns and plates. Similarly, attempts to classify snow on the ground (metamorphosed snow) were made using classical optical techniques (Colbeck 1986, Sommerfield 1969). To standardize the terminology and to seek general agreement on a classification system for new and metamorphosed snow, international committees presented The International Classification for Seasonal Snow on the Ground (Colbeck *et al.* 1990, ICSI 1954). This system, which is widely used today, describes fresh falling snow as single class that can be subdivided into eight subclasses consisting of columns, needles, plates, stellar dendrites, irregular crystals, graupel, hail, and ice pellets. Metamorphosed snow, which is considerably more complex, is described in eight distinct classes each of which has two or more subclasses. This nomenclature can be easily applied to the diverse crystal types that are found on the surface and within the three types of snowpacks that were sampled in our study, which provides greater resolution of the fresh and metamorphosed snow crystals as well as the degree of bonding that exists between adjacent grains.

### Low-Temperature Scanning Electron Microscopy Observations

The LTSEM has been previously used to describe isolated samples of metamorphosed snow crystals (Dominé *et al.* 2001, 2003; Foster *et al.* 1996; Rango *et al.* 1996b; Wergin *et al.* 1996a, b, c). The LTSEM observations by Dominé *et al.* (2003) confirm earlier conclusions (Colbeck 1983a, b, 1986; Nelson 1998; Nelson and Baker 1996; Nelson and Knight 1998), which are based on light microscopic and hand lens studies indicating that the fast growth rates probably lead to crystals with flat surfaces and sharp angles; however, hollow or concave faces can also result. The moderate growth rates produce crystals with flat faces but rounded edges. Although Dominé *et al.* (2003) also observed that even with slow to moderate metamorphism, when rounded edges were common, flat faces, sharp angles, and hollow faces could be observed, suggesting that growth rates can be very heterogeneous. Our results support this conclusion and suggest that even though the depth of the snow cover can vary considerably (from 28 cm in the Prairie to 110 in the Alpine), depth hoar crystals with sharply defined faces and flat surfaces can be found.

### Significance of Metamorphism Studies

The importance of understanding the structure and metamorphism of crystals in the snow cover has been recently

reviewed by Dominé *et al.* (2003). Briefly, the structure of snow crystals is important in quantifying the interactions between the snow cover, soils, and vegetation (Boone and Etchevers 2001), as well as in predicting the duration of snow cover (Tappeiner *et al.* 2001). Metamorphism also influences the mechanical properties of the snowpack (Durand *et al.* 1999), a feature that is important in avalanche studies (Armstrong and Armstrong 1987). In our study, the presence of a layer of loosely bonded, three-dimensional depth hoar crystals that developed at the base of the Alpine snow cover helps explain why accumulating snow fields on steep inclines ( $>45^\circ$ ) may reach a point at which the base no longer supports the weight of the accumulating snowpack. As a result, a slab avalanche, consisting of the upper portion of the snow cover, slides down the slope on the underlying depth hoar crystals that act as the “ball bearings.”

Snow crystal size and shape also affect the radiative properties or albedo of the snowpack (Schwander *et al.* 1999). For example, they influence natural microwave signals that are used for satellite remote sensing studies to predict SWE in the winter snowpack (Foster *et al.* 2005). Satellite microwave instruments (e.g., SMMR, SSM/I, AMSR-E) are being used to estimate SWE at regional and global scales. However, these estimates of SWE are sensitive to the physical properties of snow, particularly crystal characteristics and density. Snow properties are often parameterized statistically, which can increase uncertainty of the SWE estimates. Few attempts have been made to represent dynamically the shape of snow crystals in satellite-based estimation methods. Those satellite sensors operating in the microwave portion of the electromagnetic spectrum, at frequencies greater than about 20 GHz, are sensitive to snow structure and especially crystal size. Large, flat faces and internal facets, which are characteristic of the depth hoar layers found in our study, tend to scatter the signal more than that of newly fallen or partially metamorphosed snow crystals. As a result, in the models that have been developed to estimate the SWE, the reduced signal (lower brightness temperature) would tend to overpredict the amount of water that actually exists in the snow cover. To ensure that remotely sensed observations are not betrayed by faulty assumptions made about the size, shape, and orientation of snow crystals within a snowpack, studies such as ours, which illustrate the degree of faceting in the depth hoar crystals, are needed to predict the degree of microwave scattering that may occur in snow covers in different climatic/vegetative regions.

The ultimate intent is to make the passive microwave algorithms (both passive and active) more physically based, as well as more dynamic, so that they will be more responsive to varying snow conditions experienced during the course of a snow season. Snow crystals collected and analyzed in situ during season-long fieldwork, as well as during planned Arctic transects (winter of 2006), will be helpful in filling in the gaps about snow metamorphosis and should ultimately improve the performance of the snow/microwave algorithms. Modeling has been useful in this regard (Foster *et al.* 1999); however, actual observations are

required both to measure accurately the crystals and to initialize growth models.

Eventually, grain or crystal size and density models will be developed and coupled to retrieval algorithms (Kelly *et al.* 2003). The baseline SWE algorithm for the NASA AMSR-E product is

$$SWE = \frac{a(Tb18H - Tb36H)}{(1 - ff)} \text{ (mm)}$$

where *Tb18H* and *Tb36H* are the AMSR-E observed brightness temperatures at 18 GHz and 36 GHz, respectively, *ff* is the pixel fractional forest cover, and *a* is a coefficient derived from radiative transfer theory that represents the average grain size of 0.3 mm and density of 300 Kg m<sup>3</sup>. These values are considered to be average for North America during mid winter. Recently, Foster and Chang (unpublished) developed a theoretical relationship between grain size and the static *a* coefficient of the Chang *et al.* (1987) SWE algorithm, which forms the basis of this algorithm.

By accurately measuring these physical snowpack variables (grain size and density, and meteorological and radiometric variables) through season-long field campaigns, we will be filling a critical research gap about snow metamorphosis and how it affects the microwave response. Ultimately this work will improve the performance of the microwave snow retrieval algorithms.

## Conclusion

Samples collected and analyzed in this study from three types of recognized snow covers, namely, prairie, taiga, and alpine, illustrate the importance of metamorphosis in snowpack evolution. Depth hoar crystals that accumulate at the base of snowpacks have been found to affect passive microwave signals strongly. Estimates of SWE are often overinflated when snowpacks are composed of mostly large crystals. Furthermore, the occurrence and amount of depth hoar that accumulates help us to understand the metamorphic changes that lead to potential avalanche conditions.

## References

- Armstrong RL, Armstrong BR: Snow and avalanche climates of the western United States: A comparison of maritime, intermountain and continental conditions. *Int Assoc Sci Hydrol Publ* 162, 281–294 (1987)
- Beckett A, Read ND: Low-temperature scanning electron microscopy. In *Ultrastructural Techniques for Microorganisms* (Eds. Aldrich HC, Todd WJ). Plenum Pub. Corp., New York (1986) 45–86
- Boone A, Etchevers P: An intercomparison for three snow schemes of varying complexity coupled to the same land surface model: Local-scale evaluation at an Alpine site. *J Hydrometeorol* 2, 374–394 (2001)
- Chang ATC, Foster JL, Hall DK: Nimbus-7 derived global snow cover parameters. *Ann Glaciol* 9, 39–44 (1987)
- Cline D, Armstrong R, Davis R, Elder K, Liston G: *CLPX-Ground: ISA Snow Pit Measurements* (Eds. Parsons M, Brodzik MJ). National Snow and Ice Data Center, Digital Media. Boulder, CO (2002, updated 2004)

- Colbeck CS: Ice crystal morphology and growth rates at low supersaturations and high temperatures. *J Appl Phys* 54, 2677–2682 (1983a)
- Colbeck SC: The theory of metamorphism of dry snow. *J Geophys Res* 88, 5475–5482 (1983b)
- Colbeck SC: Classification of seasonal snow cover crystals. *Water Resources Res* 22, 59S–70S (1986)
- Colbeck S, Akitaya E, Armstrong R, Gubler H, Lafeuille J, Lied K, McClung D, Morris E: *The International Classification for Seasonal Snow on the Ground*. International Commission on Snow and Ice (IAHS). World Data Ctr Glaciol, Univ Colorado, Boulder, CO (1990)
- Dominé F, Cabanes A, Taillandier A-S, Legagneux L: Specific area of snow samples determined by CH<sub>4</sub> absorption at 77 K, and estimated by optical microscopy and scanning electron microscopy. *Environ Sci Technol* 35, 771–780 (2001)
- Dominé F, Lauzier T, Cabanes A, Legagneux L, Kuhs WF, Techmer K, Heinrichs T: Snow metamorphism as revealed by scanning electron microscopy. *Microsc Res Tech* 62, 33–48 (2003)
- Durand Y, Giraud G, Brun E, Merindol L, Martin E: A computer-based system simulating snowpack structures as a tool for regional avalanche forecasting. *J Glaciol* 45, 469–484 (1999)
- Erbe EF, Rango A, Foster J, Josberger EG, Pooley C, Wergin WP: Collecting, shipping, storing and imaging snow crystals and ice grains with low temperature scanning electron microscopy. *Microsc Res Tech* 62, 19–32 (2003)
- Foster JL, Hall DK, Chang ATC, Rango A, Wergin W, Erbe E: Observations of snow crystal shape in cold snowpacks using scanning electron microscopy. *Proc Internat Geosci Remote Sens Soc* 4, 2011–2013 (1996)
- Foster JL, Hall DK, Chang ATC, Rango A, Wergin W, Erbe E: Effects of snow crystal shape on the scattering of passive microwave radiation. *IEEE Trans Geosci Remote Sens* 37, 1165–1168 (1999)
- Foster JL, Sun C, Walker JP, Kelly R, Chang ATC, Dong J, Powell H: Quantifying the uncertainty in passive microwave snow water equivalent observations. *Remote Sens Environ* 94, 187–203 (2005)
- Hellman G: *Schneekristalle*. J. Muckenberger, Berlin, Germany (1893)
- ICSI: *The International Classification for Snow*. IAHS International Commission on Snow and Ice. Technical Memorandum No. 31, Associate Committee on Soil and Snow Mechanics. National Research Council, Ottawa, Canada (1954)
- Kelly R, Chang ATC, Tsang L, Foster JL: Development of a prototype AMSR-E global snow area and snow volume algorithm. *IEEE Trans Geosci Remote Sens* 41, 230–242 (2003)
- Nelson J: Sublimation of ice crystals. *J Atmospheric Sci* 55, 910–919 (1998)
- Nelson H, Baker MB: New theoretical framework for studies of vapor growth and sublimation of small ice crystals in the atmosphere. *J Geophys Res* 101, 7033–7047 (1996)
- Nelson J, Knight C: Snow crystal habit change explained by layer nucleation. *J Atmos Sci* 55, 1452–1465 (1998)
- Nordenskiöld G: The inner structure of snow crystals. *Nat Land* 48, 592–594 (1893)
- Rango A, Foster J, Josberger E, Erbe EF, Pooley C, Wergin WP: Rime and graupel: Description and characterization as revealed by low temperature scanning electron microscopy. *Scanning* 25, 121–131 (2003)
- Rango A, Martinec J, Chang ATC, Foster JL: Average areal water equivalent of snow in a mountain basin using microwave and visible satellite data. *IEEE Trans Geosci Remote Sens* 27, 740–745 (1989)
- Rango A, Wergin WP, Erbe EF: Snow crystal imaging using scanning electron microscopy: Part I. Precipitated snow. *Hydrol Sci J* 41, 219–233 (1996a)
- Rango A, Wergin WP, Erbe EF: Snow crystal imaging using scanning electron microscopy: Part II. Metamorphosed snow. *Hydrol Sci J* 41, 235–250 (1996b)
- Schwander H, Mayer B, Ruggaber A, Albold A, Seckmeyer G, Koepke P: Method to determine snow albedo values in the ultraviolet for radiative transfer modeling. *Appl Opt* 38, 3869–3875 (1999)
- Sommerfield RA: Classification outline for snow on the ground. *U.S. Forest Service–Rocky Mountain Forest and Range Experiment Station. Research paper RM-48* Fort Collins, Colorado (1969)
- Sturm M, Holmgren J, Liston GE: A seasonal snow cover classification system for local to global applications. *Amer Meteorol Soc* 8, 1261–1283 (1995)
- Tappeiner U, Tappeiner G, Aschenwald J, Tasser E, Ostendorf B: GIS-based modeling of spatial pattern of snow cover duration in an alpine area. *Ecol Model* 138, 265–275 (2001)
- UNESCO/IASH/WMO: Seasonal snow cover. *UNESCO/Int Assoc Sci Hydrol/World Meteorol Org* Paris, France (1970)
- Wergin WP, Erbe EF: Increasing resolution and versatility in low temperature conventional and field-emission scanning electron microscopy. *Scan Microsc* 5, 927–936 (1991)
- Wergin WP, Erbe EF: Snow crystals: Capturing snow flakes for observation with the low temperature scanning electron microscope. *Scanning* 16, IV88–IV89 (1994a)
- Wergin WP, Erbe EF: Use of low temperature scanning electron microscopy to examine snow crystals. *Proc 13th Internat Cong Electron Microsc* 3B, 993–994 (1994b)
- Wergin WP, Erbe EF: Can you image a snowflake with an SEM? Certainly! *Proc Royal Microsc Soc* 29, 138–140 (1994c)
- Wergin WP, Rango A, Erbe EF: Observations of snow crystals using low temperature scanning electron microscopy. *Scanning* 17, 41–49 (1995)
- Wergin WP, Rango A, Erbe EF: The structure and metamorphism of snow crystals as revealed by low temperature scanning electron microscopy. *Proc Eastern Snow Conf* 53, 195–204 (1996a)
- Wergin WP, Rango A, Erbe EF: Metamorphism of snowflakes as observed with low-temperature scanning electron microscopy. *Scanning* 18, 199–200 (1996b)
- Wergin WP, Rango A, Erbe EF, Murphy CA: Low temperature SEM of precipitated and metamorphosed snow crystals collected and transported from remote sites. *J Microsc Soc Amer* 2, 99–112 (1996c)
- Wergin WP, Rango A, Foster J, Erbe EF, Pooley C: Irregular snow crystals: Structural features as revealed by low temperature scanning electron microscopy. *Scanning* 24, 247–256 (2002)
- Wergin WP, Rango A, Foster J, Josberger EG, Erbe EF, Pooley C: Imaging and characterizing fresh and metamorphosed snow crystals with low temperature scanning electron microscopy. *Recent Res Develop Geophys* 5, 21–55 (2003)
- Wolff EW, Reid AP: Capture and scanning electron microscopy of individual snow crystals. *J Glaciol* 40, 195–197 (1994)